

# Self-Healing and Light-Soaking in MAPbI<sub>3</sub>: The Effect of H<sub>2</sub>O

*Davide Raffaele Ceratti,\* Ron Tenne, Andrea Bartezzaghi, Llorenç Cremonesi, Lior Segev, Vyacheslav Kalchenko, Dan Oron, Marco Alberto Carlo Potenza, Gary Hodes,\* and David Cahen\**

The future of halide perovskites (HaPs) is beclouded by limited understanding of their long-term stability. While HaPs can be altered by radiation that induces multiple processes, they can also return to their original state by “self-healing.” Here two-photon (2P) absorption is used to effect light-induced modifications within MAPbI<sub>3</sub> single crystals. Then the changes in the photodamaged region are followed by measuring the photoluminescence, from 2P absorption with 2.5 orders of magnitude lower intensity than that used for photodamaging the MAPbI<sub>3</sub>. After photodamage, two brightening and one darkening process are found, all of which recover but on different timescales. The first two are attributed to trap-filling (the fastest) and to proton-amine-related chemistry (the slowest), while photodamage is attributed to the lead-iodide sublattice. Surprisingly, while after 2P-irradiation of crystals that are stored in dry, inert ambient, photobrightening (or “light-soaking”) occurs, mostly photodarkening is seen after photodamage in humid ambient, showing an important connection between the self-healing of a HaP and the presence of H<sub>2</sub>O, for long-term steady-state illumination, practically no difference remains between samples kept in dry or humid environments. This result suggests that photobrightening requires a chemical-reservoir that is sensitive to the presence of H<sub>2</sub>O, or possibly other proton-related, particularly amine, chemistry.

## 1. Introduction

Halide perovskites (HaPs) have been studied widely in recent years as active materials in thin film solar cells and light-emitting diodes and as radiation detectors. The most striking characteristics of these materials are the ease with which they can be synthesized and the high quality of devices made with them. These features can be related to the materials' lattice dynamics, which, in turn can be related to the nature of their chemical bonding.<sup>[1–4]</sup> These dynamics are expressed in low frequency Raman spectra<sup>[5]</sup> and in their stability.

Usually, when a material for electronics is synthesized, it is necessary to take particular care to avoid the formation of (non-equilibrium) defects which affects the material's function negatively. However, if the bonding framework is sufficiently dynamic, the material can effectively “clean” itself from defects.<sup>[6]</sup> Because of this, the material will not

D. R. Ceratti, V. Kalchenko, G. Hodes, D. Cahen  
Department of Materials and Interfaces  
Weizmann Institute of Science  
Rehovot 7610001, Israel  
E-mail: gary.hodes@weizmann.ac.il; david.cahen@weizmann.ac.il


D. R. Ceratti  
CNRS  
UMR 9006  
IPVF  
Institut Photovoltaïque d'Île-de-France  
18 Boulevard Thomas Gobert, Palaiseau 91120, France  
E-mail: davide.ceratti@cnrs.fr

R. Tenne, D. Oron  
Department of Physics of Complex Systems  
Weizmann Institute of Science  
Rehovot 7610001, Israel

A. Bartezzaghi  
Institute of Mathematics  
École Polytechnique Fédérale de Lausanne  
Station 8, Lausanne CH-1015, Switzerland

L. Cremonesi, M. A. C. Potenza  
Department of Physics and CIMAINA  
University of Milan  
via Celoria, 16, Milan 20133, Italy

L. Segev  
Department of Physics Core Facilities Lab Automation Software Unit  
Weizmann Institute of Science  
Rehovot 7610001, Israel

 The ORCID identification number(s) for the author(s) of this article can be found under <https://doi.org/10.1002/adma.202110239>.

© 2022 The Authors. Advanced Materials published by Wiley-VCH GmbH. This is an open access article under the terms of the Creative Commons Attribution-NonCommercial License, which permits use, distribution and reproduction in any medium, provided the original work is properly cited and is not used for commercial purposes.

DOI: 10.1002/adma.202110239

require particular care in the synthesis, because it transforms rapidly into its most stable form with defect densities that can approach the thermodynamically dictated ones.

In the case of the MAPbI<sub>3</sub>, this “dynamicity” was identified, and experimentally observed<sup>[2,7]</sup> and finally confirmed by density functional theory (DFT) calculations.<sup>[8]</sup> This dynamic nature implies that one should not consider classic, static defects but rather a more complicated dynamic state.<sup>[4,9,10]</sup> Having the material in such a state could help explain phenomena such as the blinking<sup>[11,12]</sup> of large HaP clusters (>10<sup>3</sup> nm<sup>3</sup>), which cannot be explained by direct Auger recombination, with a particular electron/hole trap physically moving, changing dynamically its energy. Its energy state would flicker continuously between inside and outside the band gap with a randomized probability, thus changing it from an efficient to an ineffective trap.<sup>[4]</sup> These dynamics also affect performance efficiency and stability of the devices made with MAPbI<sub>3</sub>.

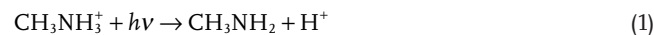
Here we show that a MAPbI<sub>3</sub> single crystal can self-heal, that is, it can return to its original state after photodamage, implying that its dynamic behavior leads the material to eliminate non-equilibrium defects. In general, light-induced modifications can cause the optoelectronic properties of the perovskite to degrade or to improve. The first process is commonly called photodamage and corresponds to the formation (or activation) of defects. The second process corresponds to the passivation or annihilation of defects and has been given various names such as “light soaking,”<sup>[13,14]</sup> “photobrightening,” and “photoenhancement.” Hereafter we will use the term photobrightening as it corresponds to an increase of the photoluminescence, PL, and photodarkening for a decrease in PL. In general, we call the process that leads to light-induced modifications in the material, as a result of exposure to strong (laser) light, photobleaching. In MAPbBr<sub>3</sub> we associated photodarkening with (transient) tri-halide interstitials<sup>[15,16]</sup> and a similar effective scheme may be involved in photodarkening of MAPbI<sub>3</sub>.

Because PL efficiency is repressed by the presence of defects with in-gap energy levels, we posit that the stronger the PL recovery after photodamage, the lower the density of optically active defects that remain in the material. While in complete cells with small-grain, polycrystalline thin films of HaPs, other mechanisms that increase the PL could take place (for example, reduction of carrier mobility that can hinder photogenerated carriers from reaching the selective contacts), in single crystals, we do not identify any alternative mechanism modifying the PL. Defect densities in thin polycrystalline films is known to be relatively low (even if some orders of magnitude less so than in single crystals), ever since the early days of PV-driven research on HaPs.<sup>[11,17,18]</sup>

The present work is distinguished from others, done on polycrystalline films (made up of crystallites of 0.5 μm average size or less), where O<sub>2</sub> can diffuse into the thin films during light treatment causing photobrightening.<sup>[11,17–19]</sup> The reason is that in our case the bleaching happens on a timescale that is too short for diffusion of chemicals from the exterior of the crystal and any effect has to be attributed to the chemicals already present in the crystal structure. We therefore study a subset of all the phenomena that can happen in a thin polycrystalline film, as found in photovoltaic and light-emitting devices. Nevertheless, our work on single crystals, is directly relevant to

thin films, because it describes effects that are present within the grains that make up these films, and as such it constitutes the benchmark for further studies with polycrystalline material.

Earlier we reported the occurrence of self-healing of photo-damage in MAPbBr<sub>3</sub>, FAPbBr<sub>3</sub>, and CsPbBr<sub>3</sub>, where all experiments were done in air with ≈45% relative humidity (RH).<sup>[15,16]</sup> Of the three Pb bromide perovskites, only MAPbBr<sub>3</sub> showed, under certain conditions, photobrightening of PL in the bulk. We explained that observation by the effect of methylamine, which will be present as a result of photolysis of methylammonium, for any given steady state, light-induced modification, according to



Illuminating MAPbI<sub>3</sub> with high, pulsed laser intensities a similar photobrightening effect is obtained. We note that in a few cases, photobrightening effects have been reported also for CsPbBr<sub>3</sub> samples. However, as those films always were obtained from either dimethyl sulfoxide (DMSO)- or *N,N*-dimethylformamide (DMF)-containing solutions, the likely cause is solvent–HaP interactions. DMF can degrade to dimethylamine and formic acid, forming dimethyl-ammonium, which can substitute partially the Cs<sup>+</sup> in the lattice and have a proton chemistry similar to methylammonium.

DMSO is known<sup>[21]</sup> to form adducts with PbBr<sub>2</sub> and can be found in CsPbBr<sub>3</sub> (as explained in the Section S0, Supporting Information). We speculate that DMSO bound to Pb<sup>2+</sup> acts like a defect, which could be passivated by photolysis breaking the Pb<sup>2+</sup>-DMSO bond. Light-induced passivation (sometimes together with oxygen) has been often invoked previously for HaPs (including Cs-based HaPs).<sup>[17,20]</sup> We note that in samples obtained from fused salts, photobrightening has not been reported for CsPbBr<sub>3</sub>.<sup>[22]</sup>

## 2. Methodology

How we visualize damage and track self-healing in the perovskite samples is particularly important for understanding the present study. For this reason, we discuss the experimental method in some detail before reporting and discussing the results.

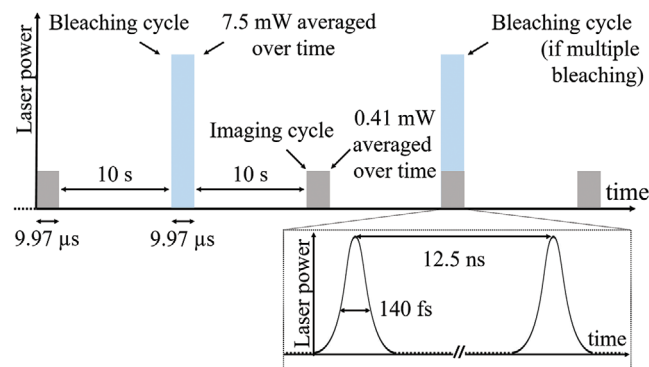
We use the PL generated by two-photon (2P) photoexcitation, ≈45 μm inside the material, thus avoiding surface-related effects. This approach is particularly important to eliminate different surfaces, due to grain boundaries, grain shapes (which can be tuned by changing the kinetics of crystallization through temperature and solvents) and due to grain and film surface defects (which can be passivated with ligands). The PL signal serves to assess the state of the material after the crystal is exposed to a high-intensity laser, similar to how we monitored self-healing in the bromide Pb perovskites.<sup>[15,16]</sup> The changes in PL, generated by the 2P upconversion of sub-bandgap radiation, reflect both damage inflicted to the MAPbI<sub>3</sub> and recovery from the damage. The experiments are done with freshly cleaved MAPbI<sub>3</sub> single crystals<sup>[23]</sup> (see below) with 2P confocal microscopy. In such microscopy a pulsed laser, emitting photons with sub-bandgap energy, 950 nm (1.305 eV) in our

case, as MAPbI<sub>3</sub> has a  $\approx 1.6$  eV band gap, which translates into an absorption onset at  $\approx 775$  nm,<sup>[24]</sup> is focused at a spot inside the crystal to reach densities sufficient to excite 2P absorption. The resulting 475 nm (2.610 eV), supra-bandgap photons generate electron–hole pairs in the MAPbI<sub>3</sub>; the recombination of these photogenerated electron–hole pairs results in the PL that is measured. To calculate the energy (density) deposited during each bleach cycle in our 2P-experiments and the penetration depth, we use the same method that is detailed in the main text and Supporting Information of our earlier report<sup>[15]</sup> (using the vectorial Debye theory).<sup>[25,26]</sup>

Cleaving the crystals assures having an almost flat surface through which the photons can enter and escape during measurement. The external surfaces of as-grown single crystals are not optically flat because of the imperfect drying process (small crystallites form from microdroplets drying on the surface of the single crystals, even if these are carefully wiped with absorbing paper). This causes “shadowing” effects inside the crystal which modify the laser intensity at the focus in the crystal, and the PL that reaches the detector.

The energy deposited at the focus inside the crystal to generate photodamage is 330 times larger than the one used for imaging (via PL excitation). The power of the damage-causing laser pulse corresponds to LP 90% (see Table S1, Supporting Information; LP = laser power). The experiment is done with the crystal (synthesis in Section S1, Supporting Information) either in dry or 45% humid N<sub>2</sub> ambient. An energy equivalent to 10 s exposure of the surface to AM 1.5 is deposited in the 10  $\mu$ s of the  $\approx 800$  pulses that make up the bleaching cycle. The energy calculation was done with the method, explained in Sections S2–S4, Supporting Information,<sup>[15,16,27]</sup> adapted to the values of 2P absorption in MAPbI<sub>3</sub> from ref. [28]. We kept 10 s between bleaching cycles to have, on average, a treatment energy equivalent to the AM1.5 solar one. **Scheme 1** illustrates all the critical parameters.

The energy deployed in this experiment is sufficient to modify the defect density in MAPbI<sub>3</sub>, but does not cause a strong increase in the local temperature. This conclusion can be intuitively evaluated considering that no modification is obtained at the low laser power (used for imaging) and that there is no material decomposition at higher laser



**Scheme 1.** Explanation of imaging and bleaching conditions: TOP: gray squares represent imaging cycles, light blue ones bleaching cycles. In both cases the cycles are composed of 798 pulses. BOTTOM: Time parameters for laser pulses to image or bleach.

powers, because the material eventually heals. In the Supporting Information (see the Charge Density and Temperature Supplementary Document, Supporting Information), we perform calculations of the expected rise in temperature and charge density at the end of the bleaching cycle. Taking into account the diffusion of the electronic charges and of heat, we find that the temperature cannot increase by more than 100 °C (i.e., up to a temperature commonly reached in the annealing steps for thin films) and that the charge density reaches a maximum of 100 $\times$  under continuous 1 sun illumination. Such a density is insufficient to induce any process other than those that can be expected to happen in operando conditions: at worst, the probability of charge recombination (induced by trap filling) is increased, which is not detrimental for the crystal and happens, even, if with lower probability, in operando. At the same time such a density is not sufficient to promote Auger recombination, which also does not happen in operando; further details are provided in the Supporting Information.

The bleaching processes happen deep inside the crystal and, therefore, photobrightening, photodamage, and self-healing can directly be attributed to the chemistry of MAPbI<sub>3</sub> (and of already existing, dissolved chemicals,<sup>[29,30]</sup> such as H<sub>2</sub>O).

Noticeably other works done on thin films reported effects on the material characteristics and/or device performance of the ambient atmosphere as, for example, O<sub>2</sub>. However, there O<sub>2</sub> actually diffuses in thin polycrystalline films (with <10  $\mu$ m grain sizes) during light treatment, increasing the photobrightening effect.<sup>[11,17–19]</sup> In our case, the bleaching happens on a timescale that is insufficient for diffusion of chemical species from the exterior (which would take several hours) implying that the effect of H<sub>2</sub>O that we find is due to the H<sub>2</sub>O already in the crystal structure.

### 3. Variability of the Data

In our experience, MAPbI<sub>3</sub> crystal growth results are much more variable than those for MAPbBr<sub>3</sub>. In films this effect of variability in properties is even stronger, as reported by Fassel et al.<sup>[31]</sup> They showed how small changes in the concentration of the precursors can affect the optoelectronic properties of MAPbI<sub>3</sub> thin films as well as the evolution of those properties under light. In the study of Fassel et al. the differences are exacerbated by possible effects of passivation and nucleation–crystallization due to passing from under- to over-stoichiometric ratio of the reagents.

Our single crystal synthesis method is the one that is most commonly used for MAPbI<sub>3</sub> and the one that is least influenced by solvent or other molecules that may enter the crystal. While there are crystallization techniques that are different from the one employed here (such as progressive degradation of NMF, N-methylformamide, by HI to form MA<sup>+</sup> in situ, causing the precipitation/crystallization<sup>[32]</sup> of MAPbI<sub>3</sub>), their use would not change the degradation and healing (chemical) mechanisms studied here as these are independent of the specific doping/defects of the crystals even if these can modify their kinetics (see Section S5, Supporting Information).

We report the results from two crystals to give an idea of the variability between samples, and so as to allow adequate

comparison of our results with literature data. We also analyzed a further ten samples briefly, with less accurate optical alignment and shorter equilibration time with the atmosphere. The reason is a very practical one, limitations on instrument availability for an extended continuous period of days and nights. Even so, those experiments showed the samples' variability by comparing the responses to the first bleaching cycles and the initial speeds of recovery. The behavior of these ten samples was intermediate between that of the two samples reported here, and for which the accurate measurements were performed and are reported. Furthermore, and importantly, *grosso modo* these two MAPbI<sub>3</sub> samples show qualitatively similar behavior. We note that there is no difference in PL emission spectra between the two crystals.

In general, our bleaching results are reproducible for any given sample in N<sub>2</sub> and each sample yields consistent results by repeating the experiment in other regions of interest in the crystal. This means that the variability is only from sample to sample and does not occur in any one sample. In a humid N<sub>2</sub> atmosphere (below 50% RH), it is necessary to wait at least 3 h to have reproducible results. For shorter times, intermediate results were found just after the bleaching which does not provide useful information for the present discussion. Drying of the crystals takes much longer than their humidification and the results continue to evolve even after 12 h (see Sections S6 and S7, Supporting Information, for further details).

As a conjecture to explain the variability between the samples we note that the doping of each crystal (which determines the Fermi level position in the bandgap) need not be the same, even for crystals, grown in the same batch. This can happen because it is unlikely that all crystals nucleate at the same time in the solution. During crystallization some I<sup>-</sup> oxidizes to I<sub>2</sub> in the solution, which leads to variation of the electrochemical (redox) potential of the solution and, therefore, of the electrochemical potential of the electrons (Fermi level) of the crystals, over time. Thus, they may have different doping densities, impacting<sup>[10]</sup> the crystal's Fermi level, especially given their relatively low doping. While normally such differences should not matter, for samples with very low doping densities as the MAPbI<sub>3</sub> crystals,<sup>[33,34]</sup> this can be an issue. If the photodamage and self-healing kinetics are influenced by the densities of free electrons and/or holes in the crystals, then this will affect the crystals' behavior after bleaching. Further details on this conjecture are provided in Section S5, Supporting Information.

#### 4. Experimental Results (Figure 1)

In **Figure 1**, we show the evolution of the 2P-generated PL of two MAPbI<sub>3</sub> single crystals (1st in black and 2nd in red) synthesized together (for the synthesis of MAPbI<sub>3</sub> single crystals, see Section S1, Supporting Information). The PL evolutions in Figure 1 are obtained after performing 100 bleaching cycles (see Scheme 1). The shaded areas indicate the time interval during which the 100 bleaching cycles occur. Each data point in the plots is obtained from a PL signal excited by 330 times lower energy than that used for photodamage. As shown in Scheme 1, the imaging cycles occur between the bleaching cycles and after the 100 bleach cycle period is over. Bleaching was under N<sub>2</sub> flow

in an inert environment (Figure 1a) or under flow of humid (45% RH) N<sub>2</sub> over the same sample that was previously imaged in dry N<sub>2</sub> (Figure 1b).

Figure 1a shows that the results in N<sub>2</sub> are quite similar for the two crystals (black and red plots). Several features, which can be attributed to different processes, are:

- Rapid initial increase (marked (1)) to  $\approx 1.3\times$  the pre-bleach value after the first bleach cycle;
- Successive bleach cycles (marked (2)) during which the PL efficiency continues to increase, up to  $\approx 2.4\times$  the pre-bleaching value after 90–100 bleaching cycles (3);
- When bleaching is stopped there is a rapid, modest PL drop to  $\approx 2.1\times$  the initial PL;
- After that the PL intensity drops slowly toward its original value with a half time of  $\approx 600$  s.

Because the long time for this stage, the main healing one, fits with a (diffusive) chemical origin, the slow PL increase (often-reported as “light-soaking” effect) has to be also of chemical origin. Our working hypothesis is that the chemical process is photolysis of MA<sup>+</sup> in MAPbI<sub>3</sub> to methylamine and H<sup>+</sup> (Equation (1)). Earlier DFT calculations showed that methylamine can bind to Pb<sup>2+</sup> in the perovskite structure, possibly donating electrons to the I–Pb–I electronic network, which defines the energies of the valence band maximum and conduction band minimum, as well as of electronically and optically active defect states.<sup>[16]</sup> In the language of electrically active defects, this process is relevant for trap filling. This effect persists until the proton re-binds to the methylamine. In this scenario, the observed effects of light-soaking and self-healing are due to acid–base, methylammonium–methylamine chemistry. While consistent with multiple results reported in the literature,<sup>[35–37]</sup> this process remains a hypothesis, direct (dis) proof of which will be hard: identifying Pb:N(H<sub>2</sub>CH<sub>3</sub>) bonds at very low concentrations (normal doping densities) during light-soaking seems beyond presently known analytical capabilities.<sup>[38]</sup> However, the results presented in the following paragraphs corroborate our hypothesis, because water is known to affect the proton chemistry in MAPbI<sub>3</sub> crystals.<sup>[39]</sup>

If, after the experiments in dry N<sub>2</sub> (Figure 1a), the MAPbI<sub>3</sub> crystals are kept in N<sub>2</sub> with 45% RH for at least 3 h before starting the experiments, the results are quite different. Figure 1b shows that pre-exposure to humidity has a very strong effect on both photobrightening and PL recovery in the bulk, even though the crystals maintain their integrity. Not only do they not change to the known yellow mono-hydrates (as happens after prolonged exposure to RH > 50% around RT),<sup>[39]</sup> also no change could be seen within our resolution, in the normal and polarized Raman spectra, PL emission spectra, or X-ray diffraction rocking curves.<sup>[40]</sup>

In humid ambient we do not observe the rapid initial PL increase (1) as in Figure 1a. While as in (2) in Figure 1a the subsequent bleach cycles increase the PL, they do so to a very limited extent. After  $\approx 12$  bleach cycles, the photoluminescence of the “black” sample peaks at  $\approx 1.15\times$  the original while the PL of the “red” sample peaks after  $\approx 30$  bleach cycles at  $\approx 1.25\times$  the original PL. Beyond that, the PL decreases for both samples (photodarkening). This behavior fits a strongly decreased

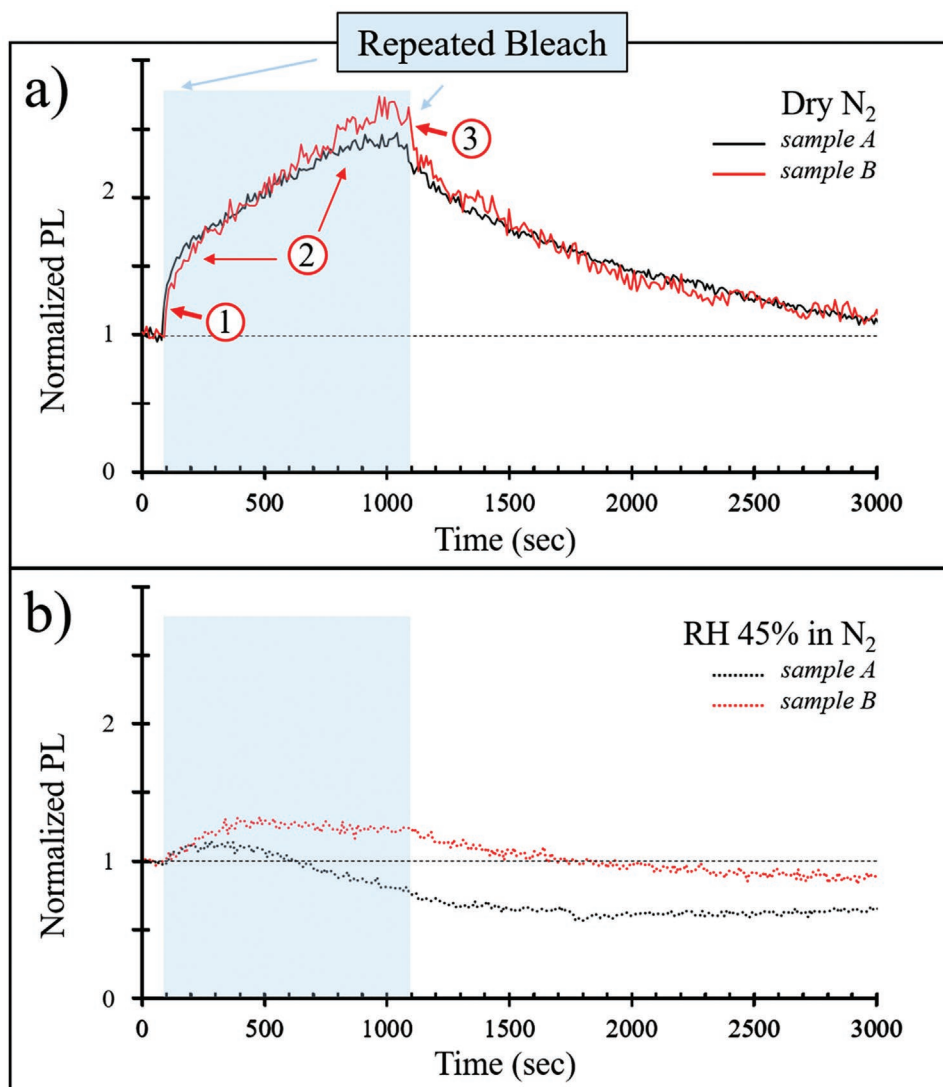


**Figure 1.** a,b) Photobleaching-induced variations of the PL from within two MAPbI<sub>3</sub> single crystals (red and black curves, normalized to the initial, i.e., pre-bleaching PL) in dry N<sub>2</sub> (a) and 45% RH in N<sub>2</sub> (b). Both plots show the time dependence of the PL as a result of up to 100 bleaching cycles (data taken in between the bleaching cycles; shown in the blue-shaded areas). Comparing plots (a) and (b) shows that water reduces the effect of photobrightening in MAPbI<sub>3</sub>. The numbers in (a) refer to stages of the PL changes, discussed in the text.

photobrightening, which allows, as the photobrightening effect decreases, photodarkening to show up.

Ignoring, for the moment, the difference in extent-time behavior of the PL change between the two samples, shown in Figure 1b, in both cases the presence of water in the ambient strongly reduces the effect of photobrightening, and that effect occurs tens of micrometers inside the crystal. This implies that water affects the internal chemistry of MAPbI<sub>3</sub> that acts against the photobrightening. During the 800 s following the end of the bleaching period both samples show similar trends. The data show that pre-exposure to humid ambient strongly inhibits the process that leads to photobrightening, which, as discussed later, might be one of the reasons why water can be so detrimental for HaP-based devices. From past reports, it can be deduced that water absorption (to be distinguished from surface adsorption<sup>[41]</sup>) in MAPbI<sub>3</sub> could be significant, from 1 H<sub>2</sub>O per

≈50–100 MAPbI<sub>3</sub> formula units to 1 H<sub>2</sub>O per 3–10.<sup>[29,30,39,42–44]</sup> It is therefore quite reasonable that water can interact, directly or indirectly with any photoinduced process and/or its product(s).

In Section S6 and Figure S2, Supporting Information, data for multiple laser powers are reported showing the same qualitative trends and differences between data collected in dry and humid N<sub>2</sub>. Samples that were pre-exposed to humidity show, after re-drying, partial recovery of the phenomena and kinetics observed under the original dry conditions (Figure S2, Supporting Information). Further details are provided in Section S6, Supporting Information.

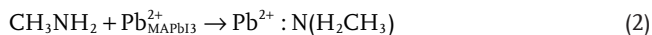
A further look at Figure 1b shows that the “black” sample accumulates more photodamage, reaching a minimum of PL (≈0.6 of the original) at around 1800 s, ≈700 s after the last photobleaching cycle. This fits with the photobrightening effect still persisting after the end of the bleach and being healed

during the post-bleaching period. Besides this, a second, slow healing of the photo-damage is present and the sample recovers part of its PL over the next 1200 s (1800–3000 s).

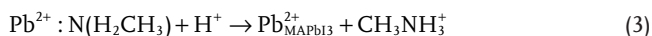
In humid ambient, the “red” sample, however, accumulates only some photodamage. Photodarkening shows after ≈1500 s and has not yet healed after 3000 s. In both samples, the processes associated with both photodamage and photobrightening take place during photobleaching. After bleaching, in both samples the products of these processes slowly react again (self-healing) to revert the material to its original state and optoelectronic properties. Even if the amount of photodamage differs between the samples, both appear to tend to a similar final state during recovery (a small recovery of the photodarkening is present in the red sample at the longest times). This shows that the processes related to photodamage, photobrightening, and self-healing of both the darkened and brightened material are relevant, regardless of the original state of the sample.

## 5. Proposed Chemical Explanation

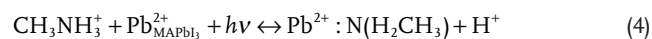
To explain the effect of water we recall the working hypothesis to explain photobrightening (Equations (1) above and (2)–(4) below) and we add the contribution of water to the over-all picture. We attribute the photobrightening to the defect-passivating coordination of Pb to the N lone-pair on CH<sub>3</sub>NH<sub>2</sub> (to form Pb:N(H<sub>2</sub>CH<sub>3</sub>)). The process starts with the above postulated photolysis of CH<sub>3</sub>NH<sub>3</sub><sup>+</sup> in the HaP (Equation (1)), followed by the formation of a Pb–N bond.



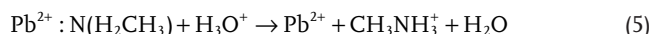
Healing happens, because, if the products cannot escape or diffuse away, Equations (1) + (2) can be reversed by H<sup>+</sup>, to reform CH<sub>3</sub>NH<sub>3</sub><sup>+</sup>:



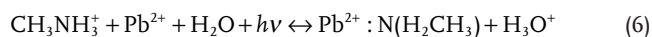
In this way a steady state is established during illumination:



Consistent with our earlier work,<sup>[39,45]</sup> where we found that H<sup>+</sup> migration in the bulk is enhanced in the presence of H<sub>2</sub>O, we find that the self-healing reaction is more rapid in more humid than in drier ambient (cf. Figure 1b with Figure 1a). This is probably because of the reaction:



and the corresponding steady state during illumination:



If we assume that the steady state for Equation (4) is more to the right than for Equation (6), we can explain why the maximum PL in dry ambient is higher than in humid ambient. This assumption can be tested by finding the energy of each configuration in the absence and presence of H<sub>2</sub>O (possibly by

future DFT calculations). One should notice that, in dry conditions, the concentration of CH<sub>3</sub>NH<sub>2</sub> is related to the amount of free H<sup>+</sup> in the lattice. Therefore, following Equation (3), if for some reason H<sup>+</sup> accumulates in the lattice, we expect the concentration of CH<sub>3</sub>NH<sub>2</sub>, determining the concentration of passivating Pb:N(H<sub>2</sub>CH<sub>3</sub>), to be lower than without such H<sup>+</sup> accumulation.

## 6. Experimental Results (Figure 2)

We now focus on the photodamage of the material that could not be properly observed in Figure 1 because of the dominating effect of photobrightening during successive bleaching cycles. To that end we look at the effects of just one bleach cycle. In Figure 2a, we show the effect on MAPbI<sub>3</sub> in dry N<sub>2</sub>. The PL increases to ≈1.3 its original value, as was the case after the first bleach cycle in the 100 bleaching cycles experiment (Figure 1a, label “1”) in both black and red samples. The PL then decreases rapidly to its original value over ≈20 s (Figure 2a, label “a”) with a decrease parallel to what happens at the end of the 100th bleaching cycle (Figure 1a, label “3”). The two samples, in black and red, differ somewhat in their behavior after that point. While the PL of the black sample decreases to ≈0.60 its original value after 600 s the red sample the minimum is reached after 1500 s with a PL of ≈0.70 its original value. Considering that the PL was still decreasing (healing of the photobrightening) after 2000 s from the end of the 100th bleaching in Figure 1a, the results of Figure 2a show that, for both samples, the recovery of the photobrightening is faster after a single bleaching cycle.

We can now draw some conclusions about the photobrightening, comparing the results from Figures 1a and 2a: in Figure 1a, we see a rapid increase (label “1”) and then a drop of around ≈0.3 times the original PL (the sharp drop, labeled “3”), respectively, after the first and after the 100th bleaching cycle. Based on the results of Figures 1a and 2a, we conclude that two different processes of photobrightening exist having different half-life times. The rapid one (≈20 s), with a PL increase of ≈0.2–0.3× the original PL, may have a physical origin (trap filling). The slow one, which can accumulate and heals more slowly (>2000 s after 100 bleach cycles and ≈600 or ≈1500 for the black and red sample respectively after 1 bleach cycle), is most probably of chemical origin.

As shown in both Figure 2a,b, and similar to what is seen in Figure 1b, the “black” sample is more affected by photodamage than the “red” one. Comparing Figure 2a,b shows that in a more humid ambient, MAPbI<sub>3</sub> is less susceptible to photodamage than in a less humid one. From these results we deduce that H<sub>2</sub>O is involved in both the photodamage process and in self-healing after photodamage.

The apparent protection that H<sub>2</sub>O conveys can be explained by considering that H<sub>2</sub>O provides extra stabilization of the Pb–I structure via H-bonds. Alternatively, H<sub>2</sub>O might deform the structure, increasing the energy needed to create (poly-) iodide interstitials. These hypotheses can be tested by DFT as formation energies of interstitials defects<sup>[4,16]</sup> and the H-bond energies can be calculated. Experimentally, if H<sub>2</sub>O deforms the structure, it would exert internal pressure; therefore, one would expect the structure to become more elastic, increasing

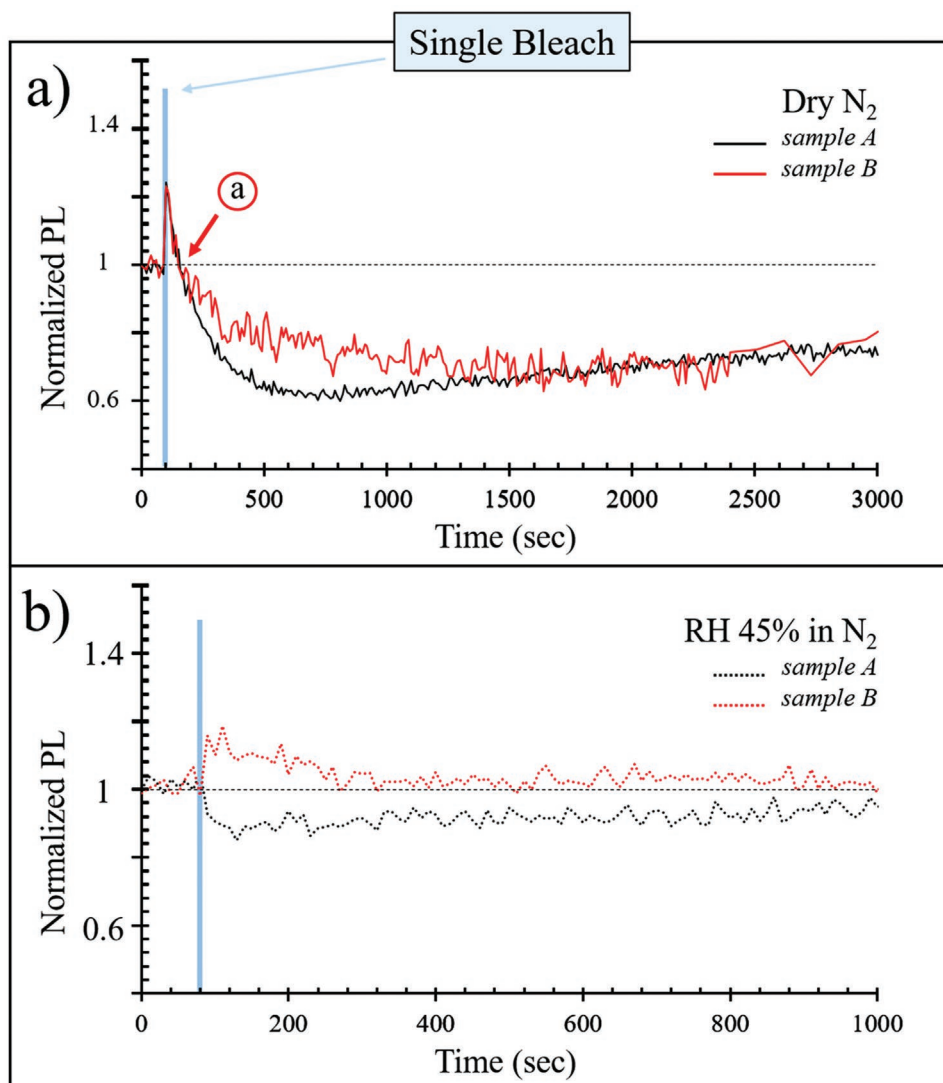


**Figure 2.** a,b) Photobleaching-induced variations of the PL from within two MAPbI<sub>3</sub> single crystals (red and black curves, normalized to the initial, i.e., pre-bleaching PL) each in dry N<sub>2</sub> (a) and 45% RH in N<sub>2</sub> (b). All plots show the time-dependence of the effect of one bleaching cycle. The time reported on the x-axis of (b) is shorter than that for (a), to allow a better view of the data.

its Young's modulus. Indeed, after exposure to humid ambient, Buchine et al.<sup>[40]</sup> found a small modulus increase for MAPbI<sub>3</sub> (and most other Pb-HaPs).

Notably, the effect of H<sub>2</sub>O does not only affect resilience to damage of MAPbI<sub>3</sub>, but also its self-healing kinetics. If the lattice is more elastic because of the presence of H<sub>2</sub>O, it can drive photogenerated distortions or defects to revert toward their original location, resulting in the healing of the material.

Putting our results and their interpretations in perspective, we note that an irradiated HaP solar cell (sealed like any (opto) electronic device) can always be considered in a steady state (on the time scale of chemical reactions) and the multiple processes that we presented will happen inside it simultaneously. Photobrightening and photodamage will be induced continually, by solar radiation, as well as the tendency of the material to attain its lowest energy state. The steady-state properties of the material can then be very different from the material's properties

just after its preparation and will likely depend on the type and extent of external inputs.

## 7. Experimental Results (Figure 3)

To get an idea of the behavior of dry and humid MAPbI<sub>3</sub> at the steady state, we checked the response of our crystals to photobleaching every 10 s causing photodamage/photobrightening over a long period of time. To that end we continued to bleach samples, up to 2200 times. In this way, the excitation and the internal chemical environment in the crystal approach, to some extent, a steady state. Indeed, the PL does not substantially vary over time anymore, despite the continuing cyclic illumination. Obviously, such an experiment cannot measure the PL in a real steady state because bleaching occurs periodically and not continuously. This is a condition imposed by both the scanning

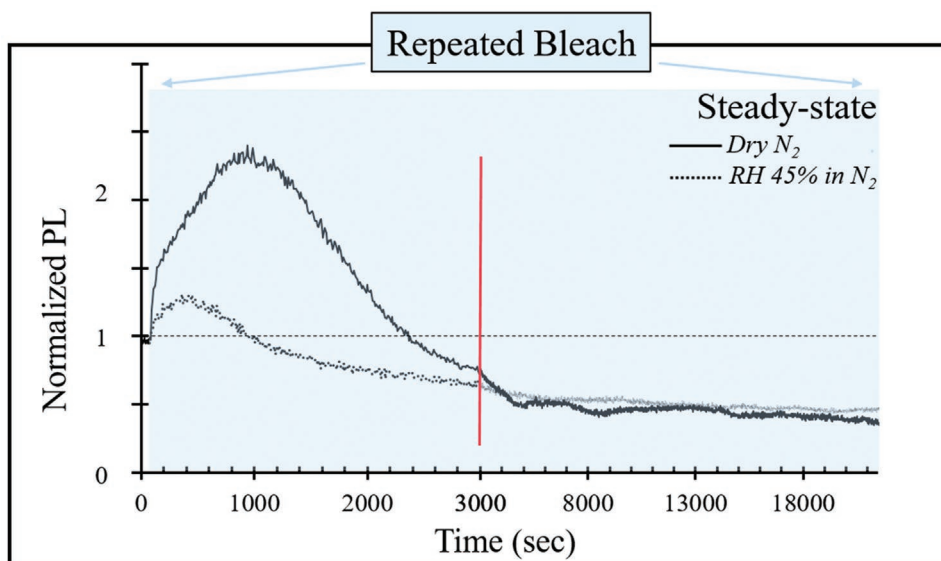


**Figure 3.** Photobleaching-induced variations of the PL of a MAPbI<sub>3</sub> single crystal, normalized to the initial, that is, pre-bleaching PL, in dry N<sub>2</sub> (full line) and in 45% RH in N<sub>2</sub> (dotted line). The bleaching is repeated 2200× to get to a quasi-steady-state. In this state (right hand side, long times) the behavior of the sample is mostly independent of humidity. The oscillations in, especially, the dry N<sub>2</sub> trace correspond to small alignment deviations due to slight variations of the laboratory ambient temperature during the experiment, which changes the focal point in the crystal. The red line shows the approximate border between the compressed (right-hand side) and extended (left-hand side) ordinate axis.

of the microscope and, especially by the use of 2P excitation, which requires a very high sub-bandgap intensity to suffice for enough nonlinear frequency doubling to get good S/N in the PL. For the same reason the laser has to be focused in the smallest possible volume. Still, our experimental settings can be viewed as a quasi-steady state given that the time of the experiment is much longer than that of a single bleaching cycle.

Analyzing the data sheds further light on the role of water. In **Figure 3**, we show the normalized PL of the first sample (black traces in Figures 1 and 2), bleached in dry N<sub>2</sub> (full line) or in humid N<sub>2</sub> (dotted line) with the same intensity of Figures 1 and 2. Up to the 100th bleach (1000 s) the results fit those shown in Figure 1. As the number of bleaches is increased further, the difference between the sample in dry N<sub>2</sub> and in humid N<sub>2</sub> decreases almost converging by the 300th bleach cycle (3000 s). At longer times (note that after 3000 s in Figure 3a, the scale of the *x*-axis changes—indicated by the red vertical line) the difference between the traces approaches zero. This shows that in this quasi-steady-state for cyclic bleaches, the external environment no longer affects the final PL, which is reduced to ≈0.45 times the original intensity.

This last result is of marked importance as it shows that some (encapsulated) samples might show very good efficiencies at short times only because of the light-soaking effects that are present in the absence of water. These will, however, eventually disappear because, as seen in Figure 3, the chemical process at the basis of photobrightening is limited in terms of how much passivation (from Equation (4)) can balance the photodamage causing a decrease of PL. Evidently, in the quasi-steady-state this process becomes less effective than initially. One interpretation of this finding is an interaction between chemical species involved in photobrightening and products of photodamage

or some slowly forming photobrightening products. Actually, in the end, after the 2200th bleach, the sample in humid N<sub>2</sub>, retains a slightly higher PL than the one in dry N<sub>2</sub>, consistent with faster self-healing of photodamage that leads to a lower (steady state) density of defects (cf. data for multiple laser powers in Section S8 and Figure S4, Supporting Information).

We note that the patterns we show in Figures 1–3 are reproduced also for a range of deployed energies between 1/20 and 1.5 times the energy reported. The corresponding data can be found in Sections S6–S8 and Figures S2–S4, Supporting Information.

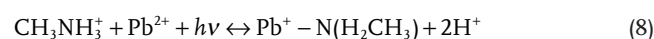
## 8. Further Chemical Mechanistic Explanation

To explain these quasi-steady-state observations, we look at possible reactions that were not previously considered, but can affect the defect equilibrium in MAPbI<sub>3</sub>. Our results can be interpreted by assuming that, over time, photobleaching produces a species that is more effective than H<sub>2</sub>O in inhibiting photobrightening. While we could not find an obvious candidate species in the literature, we can propose a plausible mechanism.

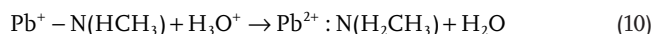
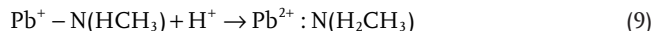
Kerner et al. showed how, in solution,<sup>[46,47]</sup> after binding to Pb, an amine can react to form a stable amide bond releasing a H<sup>+</sup> and that the process is likely to happen also in MAPbI<sub>3</sub> to form methylamide:<sup>[48]</sup>



which builds up to a steady state during illumination:



Such a steady state will not change substantially by the likely change in  $H^+$  diffusion kinetics in the presence of  $H_2O$ . The reason is that Equation (7) can be reversed, possibly with  $H_2O$ :



and that Equations (9) and (10) have probably similar activation energies, related to the breaking of the  $Pb^+ - N$  bond. If both Equations (9) and (10) are much slower than Equations (3) and (5) which re-form methylammonium, then Equations (9) and (10) determine the steady state. Kerner et al. found Equation (7) to be slow,<sup>[46]</sup> which implies that the steady state can be reached after a long time only; this can explain why convergence of the PL signals of the dry and humid sample is obtained only after hours (Figure 3). Examining the results equivalent to the ones shown in Figure 3, using lower and higher laser powers (Figure S4, Supporting Information), we could find only small differences between the data collected in humid and dry environments in the semi-steady state confirming that our observation is not power or charge concentration dependent.

## 9. Summary

We have analyzed the effect of photobleaching in the bulk of MAPbI<sub>3</sub> single crystals using PL in a 2P confocal microscope setting. Using this strategy, we avoid any material loss, allowing us to identify two types of photobrightening (light-soaking), each of which show self-healing (recovery from higher intensity to the status quo ante), with half-times around 20 and 600 s. We discovered that  $H_2O$ , absorbed in low concentrations in the perovskite bulk, hinders photobrightening, which implies that  $H_2O$  influences what is called in the literature “light-soaking” (a process that is mostly used to improve the photoconversion efficiency of HaP solar cells and contributes to reaching record efficiencies in cells that always contain some small fraction of MA). We attribute the effect of  $H_2O$  to the modification of the proton chemistry in the MA HaP, linked to the equilibrium between methylammonium and methylamine (which can bind to  $Pb^{2+}$ ). We propose a chemical mechanism involving the formation of methylamide, covalently bound to  $(Pb_{MAPbI_3})^{2+}$ , which will be affected by the proton concentration in the HaP.

We also found that  $H_2O$  modifies the process that causes photodarkening in MAPbI<sub>3</sub>, reducing the extent of damage due to the illumination and increasing the rate of the self-healing.

These results are very relevant and significant for explaining the effect of  $H_2O$  on MAPbI<sub>3</sub>. While  $H_2O$  is commonly thought to damage HaPs, in a few cases it has been reported to improve the performance of devices made with HaPs.<sup>[44,49,50]</sup>

$H_2O$  “damages” samples which are more prone to experience photobrightening. We found that  $H_2O$  increases the rate of self-healing, thus acting against photobrightening. The photobrightening is therefore reduced and the material has a lower PL compared to a sample without  $H_2O$ . At the same time, in samples where the photobrightening is weaker and photodarkening dominates,  $H_2O$  appears to improve the material, because increasing the rate of self-healing acts against photodarkening,

that is, the samples have a higher PL than if  $H_2O$  is absent. Differences between samples in the literature are probably due to different processing procedures that result, among other things, in differences in the proton chemistry between samples.

We conclude by noting that repeating the bleaching >2000 times (with an energy deposited on the sample, on average, similar to one sun) over 20,000 s ( $\approx 5.5$  h), the material reached a quasi-steady-state, where, despite the fact that the light exposure is not continuous, no further change in PL emission over time is observed. The final state is, however, almost independent of the presence of  $H_2O$ , which we explain by the formation of a chemical steady state, based on the presence of ( $Pb^+$ -amide) species, which is not affected by  $H_2O$ .

## 10. Experimental Section

MAPbI<sub>3</sub> single crystals were grown, by modifying established procedures, as follows:  $CH_3NH_3I$  and  $PbI_2$  were dissolved in  $\gamma$ -butyrolactone (GBL) at 1.1 and 1.0 M concentration respectively at 60 °C. The solution was then placed in an open crystallizer and its temperature was slowly increased to 110 °C over 3 h. Maintaining the same temperature, the solution was evaporated over time (depending on the size of the crystallizer). It was extremely important to stop the crystallization process before the complete drying of the solutions. If this was not done, multiple small crystals form on the surface of the earlier-formed large ( $\approx 1$  cm) size ones. Also, trying to redissolve and recrystallize these crystals became impossible, because they partially degrade. Indeed, upon redissolution in GBL a reddish solution was obtained that does not produce crystals with the aforementioned procedure. The identity of the species that gave the reddish color to these solutions was not investigated further.

Details on the 2P imaging in the crystal and on the evaluation of the quantification of the energy deployed locally by the light beam could be found in an earlier report<sup>[15]</sup> and in the Sections S2 and S3, Supporting Information. Refer to Section S9, Supporting Information, for the settings of the current experiments. The laser power was modulated between the imaging (5% of the maximum LP 100% = 8.2 mW) and the bleaching (90% of the maximum laser power for the data in the main text) with an increase of deployed energy of  $\approx 325$  times ( $= (90/5)^2$ ). Importantly, it was noted that the bleaching procedure did not cause heat damage inside the crystal and the effects that were analyzed were photoeffects. In this study, 2P measurements were performed either in dry or in humid  $N_2$  with a RH of 45% that was achieved by bubbling  $N_2$  through a saturated  $K_2CO_3$  solution in  $H_2O$ . The temperature was maintained around 25 °C by the facility temperature control where the microscope was placed. The amount of  $H_2O$  effectively absorbed by the single crystals were quantified in another work currently submitted to publication<sup>[42]</sup> with values around one  $H_2O$  molecule every three MAPbI<sub>3</sub> unit cells.

## Supporting Information

Supporting Information is available from the Wiley Online Library or from the author.

## Acknowledgements

The authors thank Dr. Sigalit Aharon for providing help with the cutting of halide perovskite single crystals for two-photon imaging. The authors also thank Dr. Gennady Uraltsev for the assistance with the calculations. This project has received funding from the European Union’s Horizon 2020 research and innovation program under the Marie Skłodowska-Curie grant agreement No. 893194. D.C. and D.O. thank the Yotam

project (via the Sustainability and Energy Research Initiative, SAERI, of the Weizmann Institute), G.H. and D.C. thank the Minerva Centre for Self-Repairing Systems for Energy & Sustainability, and the CNRS-Weizmann program for support.

## Conflict of Interest

The authors declare no conflict of interest.

## Data Availability Statement

The data that support the findings of this study are available in the supplementary material of this article.

## Keywords

halide perovskites stability, light-soaking, self-healing, self-repair, water

Received: December 15, 2021

Revised: May 23, 2022

Published online: July 29, 2022

- [1] A. C. Ferreira, A. Létoublon, S. Paofai, S. Raymond, C. Ecolivet, B. Rufflé, S. Cordier, C. Katan, M. I. Saidaminov, A. A. Zhumekenov, O. M. Bakr, J. Even, P. Bourges, *Phys. Rev. Lett.* **2018**, *121*, 085502.
- [2] Y. Rakita, S. R. Cohen, N. K. Kedem, G. Hodes, D. Cahen, *MRS Commun.* **2015**, *5*, 623.
- [3] A. Marronnier, G. Roma, S. Boyer-Richard, L. Pedesseau, J.-M. Jancu, Y. Bonnassieux, C. Katan, C. C. Stoumpos, M. G. Kanatzidis, J. Even, *ACS Nano* **2018**, *12*, 3477.
- [4] A. V. Cohen, D. A. Egger, A. M. Rappe, L. Kronik, *J. Phys. Chem. Lett.* **2019**, *10*, 4490.
- [5] R. Sharma, M. Menahem, Z. Dai, L. Gao, T. M. Brenner, L. Yadgarov, J. Zhang, Y. Rakita, R. Korobko, I. Pinkas, A. M. Rappe, O. Yaffe, *Phys. Rev. Mater.* **2020**, *4*, 051601.
- [6] Y. Rakita, I. Lubomirsky, D. Cahen, *Mater. Horiz.* **2019**, *6*, 1297.
- [7] S. Sun, Y. Fang, G. Kieslich, T. J. White, A. K. Cheetham, *J. Mater. Chem. A* **2015**, *3*, 18450.
- [8] M. Faghinasiri, M. Izadifard, M. E. Ghazi, *J. Phys. Chem. C* **2017**, *121*, 27059.
- [9] S. G. Motti, D. Meggiolaro, S. Martani, R. Sorrentino, A. J. Barker, F. D. Angelis, A. Petrozza, *Adv. Mater.* **2019**, *31*, 1901183.
- [10] D. Meggiolaro, S. G. Motti, E. Mosconi, A. J. Barker, J. Ball, C. A. R. Perini, F. Deschler, A. Petrozza, F. D. Angelis, *Energy Environ. Sci.* **2018**, *11*, 702.
- [11] Y. Tian, A. Merdasa, E. Unger, M. Abdellah, K. Zheng, S. McKibbin, A. Mikkelsen, T. Pullerits, A. Yartsev, V. Sundström, I. G. Scheblykin, *J. Phys. Chem. Lett.* **2015**, *6*, 4171.
- [12] A. Merdasa, Y. Tian, R. Camacho, A. Dobrovolsky, E. Debroye, E. L. Unger, J. Hofkens, V. Sundström, I. G. Scheblykin, *ACS Nano* **2017**, *11*, 5391.
- [13] M. V. Khenkin, K. M. Anoop, I. Visoly-Fisher, S. Kolusheva, Y. Galagan, F. Di Giacomo, O. Vukovic, B. R. Patil, G. Sherafatipour, V. Turkovic, H.-G. Rubahn, M. Madsen, A. V. Mazanik, E. A. Katz, *ACS Appl. Energy Mater.* **2018**, *1*, 799.
- [14] C. Zhao, B. Chen, X. Qiao, L. Luan, K. Lu, B. Hu, *Adv. Energy Mater.* **2015**, *5*, 1500279.
- [15] D. R. Ceratti, Y. Rakita, L. Cremonesi, R. Tenne, V. Kalchenko, M. Elbaum, D. Oron, M. A. C. Potenza, G. Hodes, D. Cahen, *Adv. Mater.* **2018**, *30*, 1706273.
- [16] D. R. Ceratti, A. V. Cohen, R. Tenne, Y. Rakita, L. Snarski, N. P. Jasti, L. Cremonesi, R. Cohen, M. Weitman, I. Rosenhek-Goldian, I. Kaplan-Ashiri, T. Bendikov, V. Kalchenko, M. Elbaum, M. a. C. Potenza, L. Kronik, G. Hodes, D. Cahen, *Mater. Horiz.* **2021**, *8*, 1570.
- [17] Y. Tian, M. Peter, E. Unger, M. Abdellah, K. Zheng, T. Pullerits, A. Yartsev, V. Sundström, I. G. Scheblykin, *Phys. Chem. Chem. Phys.* **2015**, *17*, 24978.
- [18] J. F. Galisteo-López, M. Anaya, M. E. Calvo, H. Míguez, *J. Phys. Chem. Lett.* **2015**, *6*, 2200.
- [19] M. Anaya, J. F. Galisteo-López, M. E. Calvo, J. P. Espinós, H. Míguez, *J. Phys. Chem. Lett.* **2018**, *9*, 3891.
- [20] S. G. Motti, M. Gandini, A. J. Barker, J. M. Ball, A. R. S. Kandada, A. Petrozza, *ACS Energy Lett.* **2016**, *1*, 726.
- [21] W. Wang, Y. Wu, D. Wang, T. Zhang, *ACS Omega* **2019**, *4*, 19641.
- [22] Y. Wang, Y. Ren, S. Zhang, J. Wu, J. Song, X. Li, J. Xu, C. H. Sow, H. Zeng, H. Sun, *Commun. Phys.* **2018**, *1*, 1.
- [23] The cleaving plane is not perpendicular to any of the crystal surfaces which makes the cleaving difficult.
- [24] A. M. A. Leguy, P. Azarhoosh, M. I. Alonso, M. Campoy-Quiles, O. J. Weber, J. Yao, D. Bryant, M. T. Weller, J. Nelson, A. Walsh, M. van Schilfgaarde, P. R. F. Barnes, *Nanoscale* **2016**, *8*, 6317.
- [25] M. Gu, in *Advanced Optical Imaging Theory*, Springer, Berlin, Germany **2000**, pp. 177–198.
- [26] M. Gu, in *Advanced Optical Imaging Theory*, Springer, Berlin, Germany **2000**, pp. 37–69.
- [27] S. Aharon, D. R. Ceratti, N. P. Jasti, L. Cremonesi, Y. Feldman, M. A. C. Potenza, G. Hodes, D. Cahen, *Adv. Funct. Mater.* **2022**, *32*, 2113354.
- [28] F. O. Saouma, D. Y. Park, S. H. Kim, M. S. Jeong, J. I. Jang, *Chem. Mater.* **2017**, *29*, 6876.
- [29] C. Müller, T. Glaser, M. Plogmeyer, M. Sendner, S. Döring, A. A. Bakulin, C. Brzuska, R. Scheer, M. S. Pshenichnikov, W. Kowalsky, A. Pucci, R. Lovrinčić, *Chem. Mater.* **2015**, *27*, 7835.
- [30] A. García-Fernández, Z. Moradi, J. M. Bermúdez-García, M. Sánchez-Andújar, V. A. Gimeno, S. Castro-García, M. A. Señaris-Rodríguez, E. Mas-Marzá, G. García-Belmonte, F. Fabregat-Santiago, *J. Phys. Chem. C* **2019**, *123*, 2011.
- [31] P. Fassl, V. Lami, A. Bausch, Z. Wang, M. T. Klug, H. J. Snaith, Y. Vaynzof, *Energy Environ. Sci.* **2018**, *11*, 3380.
- [32] J. Shamsi, A. L. Abdelhady, S. Accornero, M. Arciniegas, L. Goldoni, A. R. S. Kandada, A. Petrozza, L. Manna, *ACS Energy Lett.* **2016**, *1*, 1042.
- [33] J. Siekmann, S. Ravishankar, T. Kirchartz, *ACS Energy Lett.* **2021**, *6*, 3244.
- [34] A. Musiienko, D. R. Ceratti, J. Pipek, M. Brynza, H. Elhadidy, E. Belas, M. Betušiak, G. Delpont, P. Praus, *Adv. Funct. Mater.* **2021**, *31*, 2104467.
- [35] D. Bogachuk, L. Wagner, S. Mastroianni, M. Daub, H. Hillebrecht, A. Hinsch, *J. Mater. Chem. A* **2020**, *8*, 9788.
- [36] B. Conings, S. A. Bretschneider, A. Babayigit, N. Gauquelin, I. Cardinaletti, J. Manca, J. Verbeeck, H. J. Snaith, H.-G. Boyen, *ACS Appl. Mater. Interfaces* **2017**, *9*, 8092.
- [37] S. R. Raga, Y. Jiang, L. K. Ono, Y. Qi, *Energy Technol.* **2017**, *5*, 1750.
- [38] It will require extremely accurate measurements on samples, large volumes of which need to be light-soaked, a requirement that is difficult to accomplish due to the high absorption coefficient of the halide perovskites.
- [39] D. R. Ceratti, A. Zohar, R. Kozlov, H. Dong, G. Uraltsev, O. Girshevitz, I. Pinkas, L. Avram, G. Hodes, D. Cahen, *Adv. Mater.* **2020**, *32*, 2002467.
- [40] I. Buchine, I. Goldian, N. P. Jasti, D. R. Ceratti, S. Cohen, D. Cahen, unpublished.

- [41] H.-H. Fang, S. Adjokatse, H. Wei, J. Yang, G. R. Blake, J. Huang, J. Even, M. A. Loi, *Sci. Adv.* **2016**, *2*, e1600534.
- [42] N. P. Jasti, G. E. Sheter, Y. Feldman, D. R. Ceratti, I. Buchine, G. S. Grader, D. Cahen, unpublished.
- [43] U.-G. Jong, C.-J. Yu, G.-C. Ri, A. P. McMahon, N. M. Harrison, P. R. F. Barnes, A. Walsh, *J. Mater. Chem. A* **2018**, *6*, 1067.
- [44] S. Xiao, K. Zhang, S. Zheng, S. Yang, *Nanoscale Horiz.* **2020**, *5*, 1147.
- [45] D. R. Ceratti, A. Zohar, G. Hodes, D. Cahen, *Adv. Mater.* **2021**, *33*, 2102822.
- [46] R. A. Kerner, T. H. Schloemer, P. Schulz, J. J. Berry, J. Schwartz, A. Sellinger, B. P. Rand, *J. Mater. Chem. C* **2019**, *7*, 5244.
- [47] J. Hu, R. A. Kerner, I. Pelczer, B. P. Rand, J. Schwartz, *ACS Energy Lett.* **2021**, *6*, 2262.
- [48] R. A. Kerner, T. H. Schloemer, P. Schulz, J. J. Berry, J. Schwartz, A. Sellinger, B. P. Rand, *J. Mater. Chem. C* **2019**, *7*, 5251.
- [49] C.-H. Chiang, M. K. Nazeeruddin, M. Grätzel, C.-G. Wu, *Energy Environ. Sci.* **2017**, *10*, 808.
- [50] X. Gong, M. Li, X.-B. Shi, H. Ma, Z.-K. Wang, L.-S. Liao, *Adv. Funct. Mater.* **2015**, *25*, 6671.